Food & Function

Linking the chemistry and physics of food with health and nutrition

Accepted Manuscript

This is an Accepted Manuscript, which has been through the Royal Society of Chemistry peer review process and has been accepted for publication.

Accepted Manuscripts are published online shortly after acceptance, before technical editing, formatting and proof reading. Using this free service, authors can make their results available to the community, in citable form, before we publish the edited article. We will replace this Accepted Manuscript with the edited and formatted Advance Article as soon as it is available.

You can find more information about Accepted Manuscripts in the Information for Authors.

Please note that technical editing may introduce minor changes to the text and/or graphics, which may alter content. The journal's standard Terms & Conditions and the Ethical guidelines still apply. In no event shall the Royal Society of Chemistry be held responsible for any errors or omissions in this Accepted Manuscript or any consequences arising from the use of any information it contains.

ROYAL SOCIETY OF CHEMISTRY

rsc.li/food-function

Full title: Hydrolysis of pea protein differentially modulates its effect on iron bioaccessibility, sulfur availability, composition and activity of gut microbial communities *in vitro*

Name(s) of Author(s)

Yianna Y. Zhang[a,b], Regine Stockmann[b], Ken Ng[a] and Said Ajlouni[a]*

Author Affiliation(s)

[a]School of Agriculture and Food, Faculty of Science, The University of Melbourne, Parkville, VIC 3010, Australia

[b]CSIRO Agriculture & Food, 671 Sneydes Road, Werribee, VIC 3030, Australia

Corresponding Author

A/Prof Said Ajlouni

School of Agriculture and Food

Faculty of Science

The University of Melbourne

Royal Parade, Parkville, Victoria 3010 Australia

The University of Melbourne, Victoria 3010 Australia

T: +61 3 8344-8620 F: +61 3 8344-5037 E: said@unimelb.edu.au

Keywords: Iron bioaccessibility, iron fortification, pea protein, plant-based proteins, gut microbiome

Abstract:

Both plant proteins and iron supplements can demonstrate high susceptibility to escape small intestinal digestion and absorption, hence are often present throughout colonic fermentation. Whilst colonic iron delivery may adversely affect the gut microbiota and epithelial integrity, nascent evidence suggests that pea proteins may possess beneficial prebiotic and antioxidant effects during gut fermentation. This study investigated the interaction between exogenously added iron and pea protein isolate (PPI) or pea protein hydrolysate (PPH) during *in vitro* gastrointestinal digestion and colonic fermentation. Results revealed that enzymatic hydrolysis mitigated the crude protein's inhibitory effects on iron solubility during small intestinal digestion. Colonic fermentation of iron-containing treatments led to an increase in iron bioaccessibility and was characterized by a loss of within-species diversity, a marked increase in members of *Proteobacteria*, and eradication of some species of *Lactobacillaceae*. Although these patterns were also observed with pea proteins, the extent of the effects differed. Only PPI displayed significantly higher levels of total short-chain fatty acids in the presence of iron, accompanied by greater abundance of *Propionibacteriaceae* relative to other treatments. Additionally, we provide evidence that the iron-induced changes in the gut microbiome may be associated with its effect on endogenous sulfur solubility. These findings highlight the potential trade-off between protein-induced enhancements in fortified iron bioaccessibility and effects on the gut microbiome, and the role of iron in facilitating colonic sulfur delivery.

1. Introduction

Iron is an essential trace element with a central role in most biological systems, notably as an enzymatic cofactor in electron transfer and catalysis. However, the poor aqueous solubility of its thermodynamically favoured form [Fe(III)] (10^{-18}M, pH 7.0) makes iron absorption a challenge in the human diet[1]. Specifically, Fe(III) is highly polar and prefers O-donor ligands, which facilitates rapid hydrolysis into insoluble oxides and hydroxides upon dissolution in fluids[2]. Upon the ingestion of dietary iron, this leads to precipitation inside the oxygen-rich environment of the human small intestine, its major absorption site. In the absence of lumenal soluble ligands for the dietary iron, only a limited fraction of the free iron becomes bioaccessible, that is, maintained in a soluble form available for absorption into the body[3].

Amongst factors related to host biology and/or inadequate intake, poor dietary iron bioaccessibility is a prevailing contributor to iron deficiency, the most prevalent micronutrient disorder worldwide[4]. Iron deficiency and the associated anaemia has long-ranging effects on health, particularly towards energy metabolism, immunity, and productivity. The condition affects approximately 40% of the population in developing countries, whom largely subsist on plant-based diets containing non-heme iron, mostly as Fe(III)[5]. Despite oral supplementation strategies being developed to combat iron deficiency, non-heme iron bioaccessibility is impeded by iron's tendency to interact with plant matrix components rendering it insoluble. Examples include plant proteins, phytate, and polyphenols[1].

Limited small intestinal iron absorption due to poor bioaccessibility or impaired mucosal uptake (e.g. during elevated immunity[6]) increases lower gut iron delivery. Colonic iron absorption is feasible but less efficient (~14% of duodenal efficacy[7]), largely attributed to the presence of the gut microbiota that limits iron uptake by the host through both competition and regulatory mechanisms[8]. An increase in intraluminal iron is linked to excessive generation of reactive oxygen species (ROS) due to the redox activity of iron in the Fenton reaction. The production of ROS give rise to a cascade of events associated with acute colonic inflammation, including cytotoxic damage from lipid, protein and DNA oxidation, and reduced systemic iron absorption from hepcidin upregulation[9]. Studies have also consistently connected increased lower gut iron supply with the replication and virulence of colonic pathogens, as well as altered short-chain fatty acid (SCFA) production patterns[7]. The quantity and ratio of gut-mediated SCFAs such as acetate, propionate and butyrate play critical roles in health; including anti-inflammatory properties, maintaining intestinal cell integrity and enhancing iron absorption[10]. This implores a need to examine SCFAs as markers of gut health during iron supplementation, where existing evidence has been mixed given variations in host state *in vivo* (e.g. during anaemia) and the iron form/dosage used[11].

Iron fortification *via* food matrices have lower bioavailability than iron oral supplements, but are also deemed safer with lower toxicity[12]. Pea (*Pisum sativum L*) proteins are commonly consumed worldwide[17], which are likely co-ingested with iron. We previously found that enzymatically produced pea protein hydrolysates (PPH) enhanced the *in vitro* small intestinal bioaccessibility of fortified Fe(III), a finding likely attributable to the release of soluble iron-binding peptides during *in vitro* digestion[13]. Subsequent characterization of the Fe(III)-binding soluble fraction revealed that the sulfur-containing amino acids Cys and Met were notably absent[14]. This was consistent with the literature that Cys and Met are generally concentrated in low-digestible albumins or insoluble residue in peas[15], which posits their likelihood for colonic delivery as fermentation substrates or targets of ROS oxidation[16]. Given some recent preliminary evidence suggesting the antioxidant and prebiotic effects of pea proteins within the gut[17], the current investigation aims to investigate the possible modulatory effects of pea protein fractions (PPI and PPH) on iron and sulfur bioaccessibility dynamics throughout digestion. This includes the biomarkers of gut health (SCFA and gut bacterial composition) during *in vitro* colonic fermentation using human faecal material as the microbiota source.

2. Materials & Methods

2.1. General reagents and equipment

Common chemicals and consumables used in the study were of reagent grade and purchased from Sigma-Aldrich (Castle Hill, Australia). Pea protein isolate (PPI) from golden field peas was acquired from Pure-Product Australia (Mascot, Australia). Protease M 'Amano' (peptidase from *Aspergillus oryzae*, activity 10,000 U/g) was provided by Wilmar Bioethanol (North Sydney, Australia). Wheat phytase (6-phytase, activity 50 U/g), α-Amylase (from *Aspergillus oryzae*, activity 150 U/mg) and pepsin (from pig gastric mucosa, activity 2500 U/mg) were purchased from Sigma-Aldrich. Pancreatin was acquired from Thermo-Fisher Scientific (Scoresby, Australia). Short-Chain Fatty acid standard mixture (#28679) was acquired from Cayman chemical (Ann Arbor, Michigan, USA). All experiments were performed in triplicate, with reagents prepared using Milli-Q water (≤18 Ω) produced in-house using a Synergy UV Millipore System (Merck Life Sciences, Bayswater, Australia).

2.2. Enzymatic hydrolysis of pea protein isolate (PPI)

PPI was hydrolyzed with the enzymes phytase and protease M as previously described[13]. In summary, a 10% (w/w) PPI dispersion containing phytase at 0.8 U/g of the PPI solids was incubated for 3 hours at 50°C (ZWYR-240, Labwit Scientific, Shanghai, China), with the pH maintained at 5.0 every hour using 1 M HCl/NaOH. Protease M was then added to the mixture at 400 U/g of PPI solids and was maintained under the same incubation conditions for an additional 3 hours, after which the enzymes were inactivated by bringing the pH to 10 using 1 M NaOH. The PPH were recovered by adjusting the pH to 5.0, prior to centrifugation at 2000 *x g* for 15 min (Allegra X-12R, Beckman Coulter, Land Cove West, Australia). The pellets were frozen at −20°C and lyophilized.

2.3. Total Nitrogen analysis

The protein contents of the PPI and PPH powders, as well as the *in vitro* digested fractions undergoing colonic fermentation were determined by the Dumas Combustion method (LECO TruMac CN, Castle Hill, Australia) at a furnace temperature of 1250°C. For the PPI and PPH powders, a triplicate of 1 g was used for analysis. The soluble supernatant and their corresponding sediments following *in vitro* small intestinal digestion were analyzed wet as individual sample replicates. All results were interpreted using a Nitrogen conversion factor of 5.51 for legumes[18].

2.4. Simulated gastrointestinal digestion

2.4.1. Preparation of soluble Fe(III)-peptide mixtures

Pea protein suspensions with or without iron were prepared as previously reported[13]. PPH and PPI were dissolved in HEPES (4-(2-hydroxyethyl)-1-piperazineethanesulfonic acid) buffer (0.1 M, pH 7.0) to a final concentration of 1% (w/v). $FeCl_3$ stock solutions were separately prepared at 15 mM. For each sample, 5 mL of the $FeCl_3$ solution (equiv. 4.19 elemental iron) was added to 10 mL of the 1% PPH or PPI, or control solutions of 0.1 M HEPES without proteins by stirring for 20 min at room temperature (RT). The final mixtures (15 mL each) were then subjected to *in vitro* digestion.

2.4.2. Simulated oral, gastric and small intestinal digestion

The harmonized static INFOGEST model was adapted with simulated oral, gastric and intestinal fluids prepared per original[19]. The same incubator for enzymatic hydrolysis was used for each of the digestion stages at 37°C. For the oral phase, 5 mL of simulated saliva (containing 4 mL electrolyte oral stock solution at 1.25x concentration, 1.5 mM $CaCl_2$ and 150 U mL^{-1} α-amylase, pH 7.0) was added to each sample, and incubated for 2 min. Gastric digestion was implemented by the addition of 9.1 mL 1.25x gastric stock solution (containing 0.15 mM $CaCl_2$ and 4000 U mL^{-1} pepsin), with 1 M HCl used to adjust pH to 3.0. The samples were incubated for 2 h, prior to terminating gastric digestion by adding 16 mL of 1.25x intestinal stock solution (containing 0.6 mM $CaCl_2$ and 250 U mL^{-1} pancreatin) and 2.5 mL of 200 mM bile, with each sample further adjusted with 1 M NaOH to reach pH 7.0. Small intestinal digestion then took place for 2 h. Subsequently, the intestinal chymes were centrifuged at 2000 *x g* for 10 minutes at 20°C, with the total supernatant removed as the small intestinal bioaccessible fraction for elemental analyses. The insoluble sediment was immediately utilized for colonic fermentation.

2.5. Simulated colonic fermentation

2.5.1. Faecal culture preparation

A fresh faecal sample from a healthy 26-year-old female was collected to prepare stock cultures within 2 h of defecation, with informed consent obtained from the subject. The donor has not received antibiotics or taken probiotics for the previous 12 months. The faecal sample was homogenized in a stomacher bag with filter lining (250 µm), in pre-N_2 flushed 0.1 M phosphate buffered saline (pH 7.0) at 1:5 w/v, with the filtered fluid collected for colonic fermentation. The relevant consent and requirements for the use of human faecal cultures have been approved by the Human Research Ethics Committee at The University of Melbourne (ID: 2056152).

2.5.2. Basal medium preparation

The fermentation medium was prepared as previously described[20], mimicking the chyme of a diversified diet. Briefly, 2.5 g each of potato starch, peptone and tryptone, 2.25 g each of KCl and yeast extract, 4.5 g NaCl, 2 g mucin, 1 g pectin, 1.5 g casein, 0.75 g $NaHCO_3$, 0.4 g L-Cysteine HCl, 0.62 g $MgSO_4 \cdot 7H_2O$, 0.5 g guar gum, 0.25 g KH_2PO_4, 0.2 g bile salts, 0.55 g $CaCl_2$ and 0.5 mL Tween 80 were suspended in 500 mL of deionised water, and autoclaved at 121°C for 40 min (3041 VD, Thermoline Scientific, Wetherill Park, Australia).

2.5.3. Batch colonic fermentation and bacterial enumeration

Colonic fermentation and bacterial enumeration procedures were adapted from previous research in our laboratory[20]. The insoluble fraction from each replicate following intestinal digestion was mixed with 2 mL of fresh faecal stock culture and 3 mL of basal medium, both prewarmed to 37°C. The samples were placed in anaerobic chambers with a Gaspak (AnaeroGen™, ThermoFisher Scientific, Scoresby, Australia), prior to flushing with N_2 gas and tightening the lids. Chambers were placed in an incubator at 37 °C at 2 *x g* for 24 h. Following fermentation, the effluent samples were centrifuged at 2000 *x g* for 10 minutes at 20°C with the soluble fraction stored at –20°C for further analyses. Total plate counts of aerobic and

anaerobic bacteria took place prior to, and after 24 h of simulated colonic fermentation using Plate Count Agar in triplicates and a spread plate technique. The incubation conditions were 37°C for 48 h under aerobic and anaerobic conditions.

2.6. Elements analysis

All samples were digested and analyzed under a 5% HNO_3 and H_2O_2 sample matrix using a Perkin Elmer 8300 DV Inductively Coupled Plasma Optical Emission Spectrometer (ICP-OES) (Glen Waverley, Australia) according to our previous work[20]. Automatic sample injection (S10) was operated by the Syngistix v3.0 software (Perkin-Elmer, Glen Waverley, Australia). Calibration curves were constructed using multi-element standards (ICP-AM-17 and ICP-AM-12 Solution A, High-purity standards, Charleston, United States). Background correction was applied with multiple emission lines viewed to check for spectral interference. Random and targeted repeat analyses were performed to provide confidence.

2.7. Short-Chain Fatty Acids (SCFAs) analyses

2.7.1. Sample preparation

The SCFAs content in the supernatant after colonic fermentation was determined by gas chromatography (Agilent gas chromatographer (GC) (7890B, California, USA) coupled to a flame ionization detector (GC-FID). The sample preparation was adapted from a methodology previously optimized for faecal liquids[21]. Briefly, 250 µL of the supernatant was acidified with 200 µL of 50% sulfuric acid (w/v) and vortexed for 1 min. Previously prepared 4-methylvalerate solution (50 µL, concentration 109.5 × 10^3 µM) in diethyl ether was then added to achieve a final sample concentration of 450 µM as an internal standard. The acidified sample was then extracted with 1 mL of diethyl ether and centrifuged for 5 min at 2800 *x g*, with the organic phase transferred into a micro-centrifuge tube. The extraction was repeated three times, with 1.5 mL final volume transferred into GC vials for analysis.

2.7.2. Gas Chromatography (GC-FID) analysis

The GC-FID was coupled with an autosampler (7693 Agilent, California, USA) and an autoinjector (G4513A Agilent, California, USA) using the analytical method adapted from Gu et al.[22]. A Nukol capillary column (15 m × 0.53 mm internal diameter with 0.5 µm film thickness, Sigma-Aldrich, Castle Hill, Australia) was used, with helium as the carrier gas at a flow rate of 6 mL/min. The initial oven temperature was 100°C for 0.5 min, ramped up at 12.5°C/min to 180°C and held for 1 min, before increasing again at a rate of 20°C/min to 200°C and holding for 10 min. The FID temperature was set at 240°C with the injection port set at 200°C. Sample injection volume was 2 µL, with a split ratio of 5:1. Standard curves of the analytical standards were prepared by serial dilutions of the SCFAs standard mixture containing acetic, propionic, *iso*-butyric, *n*-butyric, *iso*-valeric and *n*-valeric acids.

2.8. Microbial profiling

2.8.1. DNA extraction, 16S rRNA gene amplification and sequencing

The baseline culture prior to fermentation, and colonic supernatant of each treatment after fermentation (200 µl per aliquot) were stored in three volumes of DNA/RNA Shield™ solution (Zymo Research, California, USA) as recommended by the manufacturer. Samples were frozen at -20°C and delivered to Australian Genome Research Facility Ltd for DNA extraction and 16S rRNA sequencing.

DNA extraction was performed using the DNeasy® PowerSoil® Pro Kit (Qiagen GmbH, Hilden, Germany). Polymerization was conducted using common primers targeting the V1-V3 region of bacterial 16S rRNA (27F 'AGAGTTTGATCMTGGCTCAG' and 519R 'GWATTACCGCGGCKGCTG'), with a read length of 300bp. The amplicons were sequenced on an Illumina MiSeq (San Diego, California, USA) platform by the MiSeq Control Software (MCS) v3.1.0.13 with Real Time Analysis (RTA) v1.18.54.4 running on the instrument computer. The Illumina DRAGEN BCL Convert 07.021.624.3.10.8 pipeline was used to generate the sequence data.

2.8.2. Taxonomic assignment

Taxonomic profiling was performed by QIIME2 as described by Bolyen et al.[23]. The demultiplexed raw reads were primer trimmed and filtered using the cutadapt plugin, followed by denoisation with DADA2[24] (*via* q2-dada2). Taxonomy was assigned to ASVs using the q2-featureclassifier[25], and clustered to operational taxonomical units (OTUs).

2.9. Data pre-processing and analyses

Bioinformatics and taxonomic visualisations were carried out with the MicrobiomeAnalyst pipeline[26] and its companion MicrobiomeAnalystR package (https://github.com/xia-lab/MicrobiomeAnalystR) unless otherwise stated. To reduce noise and low-level contamination for downstream analysis, the sequenced raw count data was filtered using the low count and low variance filters available through the platform, where a combined total of 32 features were removed. The prevalence filter was set to retain values where 10% of each OTU had >5 counts, whereas the variance filter removed features that are close to constant throughout the experiment conditions (cut-off: 10% interquartile range). Subsequent to data filtering, a rarefaction curve was generated to evaluate the adequacy of sampling depth.

The filtered raw count data were normalized using relative log-expression (RLE) for further analyses. Most microbial differential analyses (alpha- and beta-diversity indices, univariate one-way analysis of variance (ANOVA) and Linear discriminant analysis effect size analysis (LEfSe)) were performed through the MicrobiomeAnalyst pipeline, with the false discovery rate (FDR) set at 0.1 based on the Benjamini-Hochberg procedures. Both alpha- and beta-diversity analysis were examined at the feature (OTU) level across treatments.

General statistical analyses were carried out with data imported into Minitab® 20 (Minitab LLC, Pennsylvania, USA). T-tests were performed on the total nitrogen data comparing each pea fraction with their iron fortified counterparts. Differences in bioaccessible iron and sulfur,

SCFAs and total viable count among samples were analyzed with univariate ANOVA, and differences in alpha-diversity indices were analyzed with two-way ANOVA. Fisher's LSD was used as the post-hoc method where applicable. Pairwise Spearman's rank correlation was performed between SCFAs, intestinal and colonic iron and sulfur, and normalized counts of significant bacterial families as identified by ANOVA. All tests for significance were two-sided at 95% confidence, with uncertainty of replicate determinations reported to two significant figures.

3. Results

3.1. Enzymatic hydrolysis of pea proteins altered the pattern of fortified iron bioaccessibility

This study analyzed the iron found in the soluble supernatant following simulated *in vitro* small intestinal digestion and colonic fermentation as a proxy for bioaccessibility, which is the amount released from the matrix that is potentially available for absorption. The iron-fortified pea hydrolysate (PPH + Fe) showed the highest solubility after small intestinal digestion at 0.53 ± 0.052 mg, or 13% of the total 4.19 mg of fortified iron (Table 1). The $FeCl_3$ control (Fe) showed comparable levels with 0.39 ± 0.10 mg iron (9.3%) being soluble. However, the addition of fortified iron as $FeCl_3$ to unhydrolyzed PPI (PPI + Fe) led to significantly ($P < 0.05$) lower iron solubility than that of the PPH + Fe, with only 0.093 ± 0.016 mg (2.2%) of the 4.19 mg of iron loaded being soluble. This indicates that the enzymatic hydrolysis of PPI mitigated its inhibitory effects on iron bioaccessibility during small intestinal digestion, and enhanced iron bioaccessibility by 5.7-fold compared to native PPI.

A fraction of the upper gut insoluble iron in PPI + Fe was released in the lower gut, where it contributed significantly ($P < 0.05$) to a higher level of soluble Fe than PPH + Fe in the colon from fermentation (PPI + Fe: 0.34 ± 0.082 mg, PPH + Fe: 0.21 ± 0.016 mg, Table 1, equivalent to 8.1% and 5.0% of the total Fe loaded). The iron salt treated sample released 0.29 ± 0.0054 mg iron during colonic fermentation, equivalent to 6.9% of the 4.19 mg iron administered. Nonetheless, PPH + Fe exhibited the highest solubility after all digestion stages at 0.74 ± 0.025 mg (17% of Fe loaded), in comparison with the iron salt at 0.68 ± 0.10 mg (16% of Fe loaded). Furthermore, the PPI + Fe showed significantly ($P < 0.05$) lower solubility at 0.43 ± 0.092 mg (10% of Fe loaded). Based on the total Fe present in each treatment prior to *in vitro* digestion, PPH + Fe, PPI + Fe and the $FeCl_3$ control had 3.6, 3.8 and 3.5 mg of iron remaining insoluble after the intestinal digestion process, respectively.

3.2. Iron fortification is linked to lower sulfur solubility

Dietary sulfur is mainly derived from thiol amino acids in proteins[27]. The $FeCl_3$ solution used in this study is technically sulfur-free (ICP-OES detection limit: 0.752 mg/L), which suggests that the sources of sulfur in this study are from the endogenous proteins present in the digestive fluids and the pea protein fractions. As shown in Table 1, the small intestinal solubility of sulfur from the pea protein derivatives were significantly lower in the presence of iron ($P < 0.05$). PPI and PPH contained 42 ± 0.73 and 40 ± 1.10 mg of soluble sulfur respectively, approximately twice of that found in PPI and PPH with iron (PPI + Fe: 24 ± 0.49 mg, PPH + Fe: 22 ± 0.57 mg), after intestinal digestion. The Fe salt control showed similar level

of soluble sulfur to samples fortified with iron (25 ± 1.50 mg), suggesting that the addition of $FeCl_3$ reduces sulfur solubility during small intestinal digestion.

Following colonic fermentation, the soluble sulfur (S) did not differ ($P > 0.05$) amongst PPI (2.8 ± 0.092 mg) and PPI + Fe (2.9 ± 0.12 mg, Table 1) treatments. However, PPH had 6.60 ± 0.18 mg of soluble sulfur, which was significantly ($P < 0.05$) higher than PPH + Fe (2.75 ± 0.11 mg) and the salt control (2.60 ± 0.015 mg). Overall, sulfur solubility from non-fortified samples (PPI: 45 ± 0.80 mg, PPH: 47 ± 1.30 mg) were significantly ($P < 0.05$) higher than those fortified with iron (PPI + Fe: 27 ± 1.50 mg, PPH + Fe: 25 ± 0.48 mg, Fe: 27 ± 0.60 mg). This was supported by Spearman's pairwise correlation analysis, which showed an inverse association between small intestinal soluble Fe (Int-Fe) with soluble S during both intestinal digestion and colonic fermentation (Colonic S and Int-S, $r=-0.598$, $P < 0.01$, Figure 1).

3.3. Iron fortification increased colonic protein delivery from pea hydrolysates

Total nitrogen analyses showed that PPI contained 70 ± 2.5 mg protein per 100 mg powder, whereas the protein content of PPH was lower at 66 ± 3.3 mg per 100 mg powder. In terms of total protein distribution following small intestinal digestion, there was no statistical difference ($P > 0.05$) between PPI (73% or 51 ± 1.5 mg soluble, 27% or 19 ± 0.54 mg insoluble) and PPI fortified with iron (71% or 50 ± 1.4 mg soluble, 29% or 20 ± 0.96 mg insoluble) out of the 100 mg powder administered. Comparatively, the soluble protein fraction in PPH fortified with Fe (67% or 45 ± 2.2 mg) was significantly ($P < 0.05$) smaller than in PPH alone (78% or 53 ± 2.3 mg). Correspondingly, the insoluble protein fraction in PPH + Fe (33 or 21 ± 1.5 mg) was significantly larger than that PPH alone (22% or 13 ± 1.8 mg). This reveals that the binding of fortified iron to PPH led to a greater fraction of its protein resisted digestion and thus delivered to the gut, which was not observed in PPI.

3.4. Changes in gut microbiome patterns and metabolites

Following 24 h of *in vitro* colonic fermentation, samples from each treatment (PPH, PPI, Fe, PPH + Fe, PPI + Fe) were collected for total viable bacterial count, SCFAs analysis and metagenome analysis by 16S rRNA sequencing (n = 3 for each treatment). Blank ferments (n = 3) were analyzed as quality controls for bacterial count and SCFA production.

3.4.1. Bacterial abundance and SCFAs

Figure 2 shows the level of anaerobic and aerobic bacteria at 8.6 and 7.1 $\log_{10}$ CFU/mL in control fermentation after 24 h, respectively, up from 5.3 and 4.3 $\log_{10}$ CFU/mL at 0 h. It also shows that the Fe treatment had significantly higher ($P < 0.05$) mean total anaerobic and aerobic bacteria than the control after 24 h of fermentation at 11 and 10 $\log_{10}$ CFU/mL, respectively. Similarly, most treatments containing pea protein fractions had significantly higher levels of total aerobic and anaerobic bacteria relative to the control at 24 h (Figure 2).

The SCFAs detected in all treatments after 24 h of fermentation included acetic, propionic and *n*-butyric acids, while *iso*-butyric acid was found in all samples except the Fe only treatment (Figure 3). The addition of iron significantly increased the mean total SCFAs in the pea protein free control (PP-free control: 0.76 mM, Fe: 1.3 mM) (Fig 3-a). Iron fortification in the PP-free blank also increased acetic acid production (Fig 3-b), but significantly reduced levels of propionic acid (Fig 3-c) and *n*-butyric acid (Fig 3-d). In contrary, iron fortification significantly reduced total SCFAs in the PPH treatment (Fig 3-a) (PPH: 1.9 mM, PPH + Fe: 1.3 mM). However,

the total SCFAs in PPI treatment were not affected ($P > 0.05$) by Fe fortification. For pea protein samples without added iron, both PPH and PPI had greater content of total SCFAs as compared to the Fe control treatment (PPI: 1.6 mM, PPH: 1.9 mM, Control: 0.76 mM).

Comparable concentrations of acetic acid were found amongst samples containing pea fractions, although iron addition decreased the acetic acid production in PPH (Fig 3-b) (PPH: 1.3 mM, PPH + Fe: 0.87 mM, $P < 0.05$). Iron fortification also significantly ($P < 0.05$) reduced levels of propionic acid in PPH (Fig 3-c) (PPH: 0.42 mM, PPH + Fe: 0.25 mM), but elevated its production in PPI (PPI: 0.30 mM, PPI + Fe: 0.41 mM). Whilst no differences were observed in *n*-butyric acid production amongst samples with pea fractions, PPH fortified with iron showed lower levels of *iso*-butyric acid than all other samples (Figure 3).

3.4.2. General trends in bacterial community profile

For microbial profiling, 426 operational taxonomical units (OTUs) were identified according to the Greengenes database after filtering for quality. The rarefaction curve generated displayed a flat plateau, indicating that increasing data volume did not lead to significant changes in the number of OTUs (Supplementary Data 1). Six phyla were observed in this study, with >98% of the sequences from *Proteobacteria, Firmicutes, Bacteroidetes, Actinobacteria, Fusobacteria* and *Chloroflexi*. Although *Firmicutes* was the dominant phyla from the unfermented baseline culture (mean abundance: 45%), *Proteobacteria* was the most abundant in all treatments following 24 h of colonic fermentation (Figure 4-a). Fe and PPH + Fe treatments had highest mean relative proportions of *Proteobacteria* (Fe: 57%, PPH + Fe: 58%), with commensurate reductions in *Firmicutes, Actinobacteria, Bacteroidetes and Fusobacteria. Actinobacteria* was highest in PPI, Fe + PPH and Fe + PPI (means: 0.97%, 0.76% and 1.7%, respectively). Highest abundance of *Firmicutes* in the fermented group was found in Fe + PPI (mean: 35%), followed by PPH (mean: 32%). *Bacteroidetes* was the most abundant in PPH (mean: 33%), whereas *Fusobacteria* as only present in Fe-containing samples including Fe, Fe + PPH and Fe + PPI (means: 0.54%, 0.87% and 0.48%, respectively).

The top 20 families and species are depicted in Figure 4-b and 4-c, respectively. Over 93% of all OTUs could be classified at the family level at the minimum. The top 10 abundant families present in all treatments were Enterobacteriaceae, *Bacteroidaceae, Veillonellaceae, Enterococcaceae, Porphyromonadaceae, Ruminococcaceae, Rikenellaceae, Bacillaceae, Lachnospiraceae* and *Coriobacteriaceae*. The family *Alcaligenaceae* was found in all treatments except in Fe, while *Lactobacillaceae* was not identified in any treatment involving fortified iron (Fe, Fe + PPH, Fe + PPI). *Propionibacteriaceae* was only present when pea protein substrates are present with iron (Fe + PPH, Fe + PPI), whereas *Erysipelotrichaceae* was detected in all but pea protein substrates with iron (Fe + PPH, Fe + PPI).

3.4.3. Richness and diversity analysis

For alpha-diversity analysis, both indices of richness (Chao1, observed species) and diversity (Simpson, Shannon and Fisher's indices) were examined across treatments (Figure 5). The degree of similarity between community structures (beta-diversity) was examined through Principal Coordinates Analysis (PCoA), based on the Bray–Curtis dissimilarity distance. Permutational multivariate analysis of variance (PERMANOVA) and analysis of group similarities (ANOSIM) were performed to evaluate the strength of compositional differences.

As shown in Figure 4-d, the amounts of the two maximum variations amongst treatments were explained by the values of the abscissa axis (PCo1, 47.1%) and ordinate axis (PCo2, 19.3%), accounting for 66.4% of total variation. The treatment groups occupied different centroids (PERMANOVA, R-squared: 0.77205, P = 0.001), with significantly higher similarity within each group than that between them (ANOSIM, P < 0.001).

Results from PCoA analyses revealed that the microbial profiles from PPH and PPI treatments responded differently to iron fortification (Figure 5). The non-fortified treatments (PPH and PPI) largely lay in the same region in the PCoA plot with negative correlations to PCo2, whilst their iron-containing counterparts have higher PCo2 values. However, whilst PPI shifted to lower PCo1 values in the presence of iron, PPH moved toward higher PCo1 values. These trends are supported by that of alpha-diversity analyses, which showed that the presence of fortified iron significantly (P < 0.05) reduced markers of observed species, Fisher index and Chao1 in PPI, with no significant effects on Shannon and Simpson indices. On the other hand, iron addition to PPH led to a significant (P < 0.05) reduction in Fisher, Simpson and Shannon indices. Together, these results suggest that whilst iron addition was linked to a general decline in both species abundance and richness when PPI was present, only the species richness was affected in the presence of PPH.

3.4.4. Differential abundance analysis

Differential analyses were conducted on the normalized abundances of the five fermented groups (Fe control, PPI, PPH, PPI + Fe, and PPH + Fe) using ANOVA and LEfSe, respectively. Results shown in Fig 6 indicated that at the minimum classification level of family, univariate ANOVA revealed that *Propionibacteriaceae* was significantly higher in treatments containing both iron and a pea protein substrate (Fe + PPH and Fe + PPI, P < 0.01). This corroborates with findings from LEfSe, which identified *Propionibacteriaceae* as a biomarker for Fe + PPI (adj-P < 0.01, LDA score: 2.47). Without fortified iron, PPI is characterized by higher levels of *Bacillaceae* (P < 0.01, LDA score: 4.27), *Bacteroidaceae* (P < 0.05, LDA score: 3.62), *Porphyromonadaceae* (P < 0.05, LDA score: 2.81), Lachnospiraceae (P < 0.05, LDA score: 2.75) and Coriobacteriaceae (P < 0.05, LDA score: 2.35) from LEfSe. These patterns were confirmed by cluster analyses and ANOVA, although the effects on *Bacteroidaceae* and *Porphyromonadaceae* were no longer significant after adjusting for FDR (P > 0.05). *Alcaligenaceae* was identified as a marker for PPH with fortified iron (P < 0.02, LDA score: 3.52), where it was notably lower in the iron control without pea protein substrates (ANOVA: P < 0.001). Iron treatment alone was characterized by *Enterobacteriaceae* and *Enterococcaceae* from LEfSe (P < 0.05, LDA Scores: 4.27 and 3.32, respectively). ANOVA analyses confirmed that *Enterococcaceae* was significantly higher in Fe relative to other treatments, although Fe was not similar in relative abundance to Fe + PPH for *Enterobacteriaceae* (P < 0.05, Figure 6).

3.5. Correlation between iron and sulfur availability and SCFAs production and bacterial taxa

3.5.1. Elements bioaccessibility and SCFAs

As shown in Figure 1, apart from its association to intestinal and colonic bioaccessible sulfur, small intestinal bioaccessible Fe (Int-Fe) was also negatively correlated with the production of all detected SCFAs except *n*-butyric (acetic, r=-0.575, P < 0.05; propionic, r=-0.651, *iso*-

butyric, r=0.821; total SCFAs, r=-0.71, P < 0.01). Similar patterns were observed for Colonic Fe, except the association was only significant for *iso*-butyric (Colonic Fe, r=-0.655, P < 0.01). Colonic S and Intestinal S were positively associated (P < 0.01) with propionic (r=0.854), isobutyric (r=0.592) and total SCFAs (r=0.693).

3.5.2. Gut community abundance and SCFAs

The normalized abundances of several bacterial families, including *Alcaligenaceae* (r=-0.588, P < 0.05), *Coriobacteriaceae* (r=-0.636, P < 0.01) and *Enterobacteriaceae* (r=-0.593, P < 0.05) demonstrated an inverse relationship with the production of acetic acid. *Enterobacteriaceae* was also negatively correlated with propionic acid (r=-0.879, P < 0.01), isobutyric acid (r=-0.564, P < 0.05) and total SCFAs (r=-0.932, P < 0.01). The only family associated *n*-butyric acid production was *Lachnospiraceae* (r=0.457, P < 0.05). Several families were positively associated with isobutyric acid with varying strengths, including *Ruminococcaceae* (r=0.566, P < 0.05), *Bacteroidaceae* (r=0.677, P < 0.05), *Lachnospiraceae* (r=0.707, P < 0.01) and *Lactobacillaceae* (r=0.826, P < 0.01).

3.5.3. Elements bioaccessibility and gut community abundance

Int-Fe was negatively associated with abundances of *Bacteroidaceae* (r=-0.585, P < 0.05), *Erysipelotrichaceae* (r=-0.682, P < 0.01), *Lachnospiraceae* (r=-0.598, P < 0.05), *Lactobacillaceae* (r=-0.843, P < 0.01) and *Ruminococcaceae* (r=-0.598, P < 0.05), but positively associated with *Enterobacteriaceae* (r=0.666, P < 0.01). Similar associations were observed with Colonic Fe for *Bacteroidaceae* (r=-0.682, P < 0.01), *Erysipelotrichaceae* (r=-0.696, P < 0.01), *Lachnospiraceae* (r=-0.732, P < 0.01), and *Lactobacillaceae* (r=-0.886, P < 0.01). Meanwhile, *Propionibacteriaceae* was positively associated with Colonic Fe (r=0.62, P < 0.05). The only family with significant association with sulfur (both Int-S and Colonic S) was *Enterobacteriaceae* (r=-0.736, P < 0.01).

4. Discussion

Hydrolysis products derived from food proteins can mediate iron bioaccessibility during digestion through multiple mechanisms, one being an increase in iron's solubility that is needed for absorption. Partially hydrolyzed proteins, peptides, and amino acids may enhance intestinal iron bioaccessibility by their ionizable groups forming low molecular weight (MW) soluble complexes with iron, thereby circumventing its polynucleation with other counterions (e.g. phosphates, oxides and hydroxides) that decreases iron solublility. Such mechanism is more convoluted in the context of legume proteins, where their affinity for iron is coupled with structures and regions that exhibit hydrolytic resistance against digestive enzymes and brush border amino peptidases[28]. Several legume proteins have been shown to inhibit fortified iron solubility, hence bioavailability, *in vivo*[29, 30], which are consistent with our findings from the native pea protein (PPI). This digestion-resistant fraction containing both legume protein and fortified iron reaches the lower gut, although their combined effects on colonic microbiome markers have been unexplored until this study.

Enzymatic hydrolysis of the pea protein prior to intestinal digestion mitigated its detrimental effect on small intestinal iron bioaccessibility during iron fortification, with a lower fraction of the soluble iron released within the gut. Such finding confirms that the inverse correlation between iron bioaccessibility and the MW of protein hydrolysates is applicable to pea proteins, given sufficient hydrolysis by both phytase and protease to achieve peptide

fragments with sufficient hydrophilicity. During gastric digestion, pea peptic products are formed *in situ* that are known inhibitors of digestive enzymes within the small intestine[31]. As such, partial unfolding of the polypeptides can increase the ionizable groups and iron-binding but restrict its bioaccessibility, due to the poorly soluble complexes formed. A parallel view of both iron bioaccessibility and protein distribution suggests that treatment of PPI by protease and phytase likely enhanced both soluble and insoluble binding iron peptides, which eventuated in improved small intestinal bioaccessibility. Referring to similar static *in vitro* gastrointestinal models employed in previous reports, the 5.7-fold increase in small intestinal iron solubility was consistent with those examining fortified iron with crude versus hydrolysed legume proteins. This includes the 5-fold increase found in our former study with pea hydrolysates[13] and the 3.5- to 6.0-fold enhancement reported in soy hydrolysates by Devaraju et al.[32]. Comparatively, the same pea hydrolysates that underwent a longer digestion period of 3 h showed a considerably higher increase in iron solubility[13]. These results reiterate the critical role of adequate legume protein digestibility in mediating iron bioaccessibility, which in *in vitro* studies may be a function of the digestion protocol conditions employed.

Iron(III) supplementation alone led to increased soluble colonic iron, which promoted conditions associated with an imbalanced microbiome and shifts in SCFA production profile. Despite the low dose of iron used in this study (4.2 mg elemental iron versus 35-65 mg/dose for treating iron deficiency anemia[12]), gut bioaccessibility for all fortified treatments exceeded the 0.4 mmol reported for conventionally accessible intraluminal iron[7]. Consistent with findings by Dostal et al.[33] in rodents, iron salt addition led to greater total SCFAs production in colon as a likely result of enhanced bacteria metabolic activity. However, we found that such increase in total SCFAs resulted in altered ratios over favouring acetate (86% of total SCFAs in Fe versus 47% in the fermented treatments without Fe), which was also observed by Poveda et al.[34]. This may be suggestive of selective enrichment in acetogenic species under iron fortification *in vitro*, which is supported by our findings of significant higher total aerobic bacteria count in the presence of Fe. Total aerobic count can indicate an increase in facultative anaerobes such as *Enterococcaceae* and *Enterobacteriaceae*, which are known acetate producers[35] and identified as LEfSe biomarkers for Fe in this study. Proliferation of the latter is associated with the depletion of butyrate-producing species[36], which hinders the ability of acetate to be utilized towards butyrate production *via* cross-feeders. Such shift affects the availability of butyrate as the source providing 70-80% of total energy for colonocytes[37], as well as a contemporaneous decline in commensal/beneficial species. At the phylum level, we observed an expansion in members of *Proteobacteria* that were most prominent in Fe amongst all treatments. The proliferation of *Proteobacteria* (particularly *Enterobacteriaceae*) has been one recurrent outcome of recent iron supplementation studies[7]. Many pathogenic and/or virulent species of *Proteobacteria* possess a growth advantage under increased iron availability, which can ultimately attenuate host colonic iron uptake *in vivo* through competition[7].

Reflecting the different composition of the digestion products, we found that iron fortification of the two pea structures led to disparate effects on the gut microbiota. Iron fortification with PPH led to decreased production of the proteolytic metabolite *iso*-butyric acid when compared to PPH alone. However, the addition of iron also significantly decreased ($P < 0.05$)

the total SCFA production and species richness found in PPH. Conversely, fortification of Fe with PPI led to a decline in both species' abundance and richness. Consistent with a significant increase in *Propionibacteriaceae*, iron addition to PPI also led to higher levels of propionic acid, resulting in the highest levels of total SCFAs amongst all treatments. Despite the baseline differences between PPI and PPH, iron fortification of either fraction led to lower gut microbial diversity compared to without. This may be linked to the loss of potentially important taxa observed in the presence of iron, such as *Lactobacillaceae*, which plays a pivotal role in regulating iron absorption *via* the production of microbial metabolites *in vivo*[8]. Nonetheless, the higher SCFAs found in presence of pea fractions may partially ameliorate the effects of fortified iron. This is as SCFAs have been proposed as mediators of colonic iron absorption[10], with low faecal concentrations observed under iron-deficient conditions in both rodents[38], and in *vitro*[39]. To date, elevated SCFAs production and an increase in the family *Ruminococcaceae* have been two of the only consistent findings regarding the effects of pea protein on the gut microbiota[17]. The latter was also observed in our study, where PPI-containing treatments contained the highest relative abundance. *Ruminococcaceae* are associated with butyrate production amongst the other biomarker families of PPI, including *Lachnospiraceae, Coriobacteriaceae* and *Porphyromonadaceae*[40].

Our findings shed lights on the prospective role of sulfur in the modulation of iron bioaccessibility from mineral salts and its subsequent effects on the gut microbiome. Analogous to *in vivo*, sulfur in this study was derived from proteins originating both endogenously (digestive fluids) and from dietary sources (pea proteins). We observed an inverse relationship between bioaccessible iron and sulfur following small intestinal digestion, where iron fortification of samples consistently decreased soluble sulfur regardless of the substrate. Although sulfur is known to be liberated from amino acids[41], the successive increase in colonic soluble sulfur in iron-fortified treatments was not followed by higher levels of soluble sulfur following fermentation. This suggests that fortified iron led to insoluble sulfur-containing fractions following intestinal digestion, which remained intact during colonic fermentation. It is also possible that surfur might be released as volatile compounds under such condition. Sulfur-rich food proteins have long been implicated in enhancement of iron bioaccessibility, owing to the ability of low MW digestion products with sulfhydryl groups to reduce Fe(III) to Fe(II) that can form more soluble iron complexes[42]. However, the high affinity of Fe(III) towards sulfhydryl and carboxyl groups can take precedence over its binding to hydroxyl groups, forming iron chelates with low solubility. Less soluble iron-sulfur chelates have been recognized in polysaccharides in reducing iron bioaccessibility[43], although there has been less discussion on the context of proteins and their effects on the gut. Recent evidence suggested that ferrous sulfate demonstrated mixed effects on rodent gut models relative to other forms of iron supplementation[44], and it remains unclear as to what extent any gut alterations may be attributed to sulfur. The ramifications of indigestible iron-sulfur complexes is worthwhile exploring, with implications for using ferrous sulfate as the gold standard for iron oral supplementation[12], as well as protein-rich sources of iron as the main source of dietary sulfur for most individuals[45].

The significant association between bioaccessible gut sulfur and *Enterobacteria* further suggests that protein-derived sulfur may be an intermediate exacerbating the effects of iron fortification during colonic fermentation. Pathogens such as *Escherichia coli* and

Pseudomonas aeruginosa have been identified to encode genes involved in the production of hydrogen sulfide (H_2S) *via* cysteine degradation[46], a process that can be further stimulated by dietary sulfur[45]. Elevated H_2S production has been implicated in the pro-inflammatory effects of high-protein diets, as well as toxic to lactic acid bacteria[47]. As such, iron-induced gut sulfur delivery may generate independent effects associated with iron (e.g. an increase in *Enterobacteria*), but also provide additional substrate for increased H_2S that possibly contribute to the obliteration of *Lactobacillaceae*. Whilst H_2S was not specifically measured in this study, we found significantly higher levels of bioaccessible gut sulfur from PPH treatment relative to PPI. This is supportive of our hypothesis that the sulfur-containing proteins from PPH are delivered to the colon with the undigested fraction, where sulfur would have been released during fermentation without the presence of fortified iron forming insoluble complexes.

5. Conclusion

The present study sheds light on the complex interrelationship between plant protein structure, digestibility, fortified iron bioaccessibility and their association with changes in the gut microbiome. Our findings were limited by the *in vitro* nature that merely reflect acute changes within an adult microbiome, which can be more stable overtime. Additionally, our analysis of the soluble faecal medium likely excluded some microbial load within the insoluble pellet that may explain the loss of some species. Nonetheless, this investigation highlights a prospective role of fortified iron to increase lower gut sulfur supply, which may be one fundamental mechanism exacerbating iron's deleterious effects on the colonic microbiota. Future studies are urged to examine the robustness of the changes in gut microbiome profile that stem from fortifying iron through pea protein matrices, amidst interindividual differences. The range of proteolytic metabolites produced should also be explored to elucidate pea proteins' putatively protective effects on the gut, particularly H_2S as a sulfur by-product.

Acknowledgements

The authors appreciate Nur Houssain, Siyao Liu, Zhenzhao Li and Yit Tao Loo for their generous assistance with the GC-FID analyses. We also thank the Melbourne TrACEES Platform (Trace Analysis for Chemical, Earth and Environmental Sciences) for the expertise received conducting the ICP-OES analyses, and to Australian Genome Research Facility Ltd. for performing the 16S rRNA sequencing and data pre-processing. Yianna Y. Zhang is a recipient of CSIRO Postgraduate Scholarship and a Research Scholarship at the University of Melbourne. Regine Stockmann acknowledges funding support from the Precision Health Future Science Platform at CSIRO.

Conflicts of interest

The authors report no conflicts of interest.

5. Tables

Table 1. Bioaccessibility distribution of iron and sulfur (in mg) from Fe salt control ($FeCl_3$) and pea protein fractions (PPI and PPH) with and without Fe fortification following *in vitro* digestion and colonic fermentation. Bioaccessibility results were expressed as means ± SD (n = 3). Means followed by different superscript letters within each column of each element differ ($P < 0.05$). Numbers in parentheses indicate the mean element concentration present within the sample excluding digestive fluids.

	Intestinal	**Colonic**	**Total bioaccessible (Intestinal + Colonic)**
Iron			
PPI (0.027)	n.d.*	0.020 ± 0.0022^{a}	0.020 ± 0.0022^{a}
PPH (0.068)	n.d.*	0.074 ± 0.025^{a}	0.074 ± 0.025^{a}
PPI + Fe (4.2)	0.093 ± 0.016^{a}	0.34 ± 0.082^{b}	0.43 ± 0.092^{b}
PPH + Fe (4.3)	0.53 ± 0.052^{b}	0.21 ± 0.016^{c}	0.74 ± 0.056^{c}
Fe control (4.2)	0.39 ± 0.10^{b}	0.29 ± 0.0054^{bc}	0.68 ± 0.10^{c}
Sulfur			
PPI (1.8)	42 ± 0.73^{a}	2.8 ± 0.092^{b}	45 ± 0.80^{a}
PPH (1.7)	40 ± 1.10^{a}	6.6 ± 0.18^{a}	47 ± 1.30^{a}
PPI + Fe (1.8)	24 ± 0.49^{b}	2.9 ± 0.12^{b}	27 ± 1.5^{b}
PPH + Fe (1.7)	22 ± 0.57^{b}	2.8 ± 0.11^{b}	25 ± 0.48^{b}
Fe control (0)	25 ± 1.50^{b}	2.6 ± 0.015^{b}	27 ± 0.60^{b}

* n.d. = below detection limit of 0.06 mg/L analyzed liquid

6. References

1. T. Ems, K. St Lucia and M. R. Huecker, *Biochemistry, Iron Absorption*, StatPearls Publishing, Treasure Island, Florida, 2017.
2. M. Sánchez, L. Sabio, N. Gálvez, M. Capdevila and J. M. Dominguez‐Vera, Iron chemistry at the service of life, *IUBMB life*, 2017, **69**, 382-388.
3. P. Etcheverry, M. A. Grusak and L. E. Fleige, Application of in vitro bioaccessibility and bioavailability methods for calcium, carotenoids, folate, iron, magnesium, polyphenols, zinc, and vitamins B6, B12, D, and E, *Frontiers in Physiology*, 2012, **3**, 1-22.
4. R. L. Bailey, K. P. West and R. E. Black, The epidemiology of global micronutrient deficiencies, *Annals of Nutrition & Metabolism*, 2015, **66**, 55-66.
5. I. G. Rusu, R. Suharoschi, D. C. Vodnar, C. R. Pop, S. A. Socaci, R. Vulturar, M. Istrati, I. Moroșan, A. C. Fărcaș and A. D. Kerezsi, Iron supplementation influence on the gut microbiota and probiotic intake effect in iron deficiency—A literature-based review, *Nutrients*, 2020, **12**, 1993.
6. T. Bartosik, S. A. Jensen, S. M. Afify, R. Bianchini, K. Hufnagl, G. Hofstetter, M. Berger, M. Bastl, U. Berger, E. Rivelles, K. Schmetterer, J. Eckl-Dorna, F. F. Brkic, E. Vyskocil, S. Guethoff, A. Graessel, M. F. Kramer, E. Jensen-Jarolim and F. Roth-Walter, Ameliorating Atopy by Compensating Micronutritional Deficiencies in Immune Cells: A Double-Blind Placebo-Controlled Pilot Study, *The Journal of Allergy and Clinical Immunology: In Practice*, 2022, **10**, 1889-1902.e1889.
7. B. Yilmaz and H. Li, Gut Microbiota and Iron: The Crucial Actors in Health and Disease, *Pharmaceuticals*, 2018, **11**, 98.
8. N. K. Das, A. J. Schwartz, G. Barthel, N. Inohara, Q. Liu, A. Sankar, D. R. Hill, X. Ma, O. Lamberg, M. K. Schnizlein, J. L. Arqués, J. R. Spence, G. Nunez, A. D. Patterson, D. Sun, V. B. Young and Y. M. Shah, Microbial Metabolite Signaling Is Required for Systemic Iron Homeostasis, *Cell Metabolism*, 2020, **31**, 115-130.e116.
9. T. S. Koskenkorva-Frank, G. Weiss, W. H. Koppenol and S. Burckhardt, The complex interplay of iron metabolism, reactive oxygen species, and reactive nitrogen species: insights into the potential of various iron therapies to induce oxidative and nitrosative stress, *Free Radical Biology and Medicine*, 2013, **65**, 1174-1194.
10. A. Soriano-Lerma, M. García-Burgos, M. J. M. Alférez, V. Pérez-Carrasco, V. Sanchez-Martin, Á. Linde-Rodríguez, M. Ortiz-González, M. Soriano, J. A. García-Salcedo and I. López-Aliaga, Gut microbiome–short-chain fatty acids interplay in the context of iron deficiency anaemia, *European Journal of Nutrition*, 2022, **61**, 399-412.
11. A. M. Puga, M. D. Samaniego-Vaesken, A. Montero-Bravo, M. Ruperto, T. Partearroyo and G. Varela-Moreiras, Iron Supplementation at the Crossroads of Nutrition and Gut Microbiota: The State of the Art. *Nutrients*, 2022, **14**.
12. S. R. Bloor, R. Schutte and A. R. Hobson, Oral Iron Supplementation—Gastrointestinal Side Effects and the Impact on the Gut Microbiota, *Microbiology Research*, 2021, **12**, 491-502.
13. Y. Y. Zhang, R. Stockmann, K. Ng and S. Ajlouni, Bioprocessing of Pea Protein can Enhance Fortified Fe But Reduce Zn In Vitro Bioaccessibility, *Journal of Agricultural and Food Chemistry*, 2022, **70**, 1241-1251.
14. Y. Y. Zhang, R. Stockmann, K. Ng, J. A. Broadbent, S. Stockwell, H. Suleria, N. E. Karishma Shaik, R. R. Unnithan and S. Ajlouni, Characterization of Fe(III)-binding peptides from pea protein hydrolysates targeting enhanced iron bioavailability, *Food Chemistry*, 2023, **405**, 134887.

15. L. A. Rubio, A. Pérez, R. Ruiz, M. Á. Guzmán, I. Aranda‐Olmedo and A. Clemente, Characterization of pea (Pisum sativum) seed protein fractions, *Journal of the Science of Food and Agriculture*, 2014, **94**, 280-287.
16. T. Hoshi and S. Heinemann, Regulation of cell function by methionine oxidation and reduction, *J Physiol*, 2001, **531**, 1-11.
17. J. Wang, S. Kadyan, V. Ukhanov, J. Cheng, R. Nagpal and L. Cui, Recent advances in the health benefits of pea protein (Pisum sativum): bioactive peptides and the interaction with the gut microbiome, *Current Opinion in Food Science*, 2022, **48**, 100944.
18. S. Fujihara, H. Sasaki and T. Sugahara, Nitrogen-to-Protein Conversion Factors for Some Pulses and Soybean Products, *Journal for The Integrated Study of Dietary Habits*, 2010, **21**, 60-66.
19. M. Minekus, M. Alminger, P. Alvito, S. Ballance, T. Bohn, C. Bourlieu, F. Carrière, R. Boutrou, M. Corredig and D. Dupont, A standardised static in vitro digestion method suitable for food–an international consensus, *Food & function*, 2014, **5**, 1113-1124.
20. Y. Y. Zhang, J. Panozzo, M. S. Hall and S. Ajlouni, Bioaccessibility of Some Essential Minerals in Three Selected Australian Pulse Varieties Using an In Vitro Gastrointestinal Digestion Model, *Journal of Food Science*, 2018, **83**, 2873-2881.
21. S. Scortichini, M. C. Boarelli, S. Silvi and D. Fiorini, Development and validation of a GC-FID method for the analysis of short chain fatty acids in rat and human faeces and in fermentation fluids, *Journal of Chromatography B*, 2020, **1143**, 121972.
22. C. Gu, K. Howell, A. Padayachee, T. Comino, R. Chhan, P. Zhang, K. Ng, J. J. Cottrell and F. R. Dunshea, Effect of a polyphenol-rich plant matrix on colonic digestion and plasma antioxidant capacity in a porcine model, *Journal of Functional Foods*, 2019, **57**, 211-221.
23. E. Bolyen, J. R. Rideout, M. R. Dillon, N. A. Bokulich, C. C. Abnet, G. A. Al-Ghalith, H. Alexander, E. J. Alm, M. Arumugam and F. Asnicar, Reproducible, interactive, scalable and extensible microbiome data science using QIIME 2, *Nature biotechnology*, 2019, **37**, 852-857.
24. B. J. Callahan, P. J. McMurdie, M. J. Rosen, A. W. Han, A. J. Johnson and S. P. Holmes, DADA2: High-resolution sample inference from Illumina amplicon data, *Nat Methods*, 2016, **13**, 581-583.
25. N. A. Bokulich, B. D. Kaehler, J. R. Rideout, M. Dillon, E. Bolyen, R. Knight, G. A. Huttley and J. Gregory Caporaso, Optimizing taxonomic classification of marker-gene amplicon sequences with QIIME 2's q2-feature-classifier plugin, *Microbiome*, 2018, **6**, 1-17.
26. J. Chong, P. Liu, G. Zhou and J. Xia, Using MicrobiomeAnalyst for comprehensive statistical, functional, and meta-analysis of microbiome data, *Nature Protocols*, 2020, **15**, 799-821.
27. M. E. Nimni, B. Han and F. Cordoba, Are we getting enough sulfur in our diet?, *Nutr Metab (Lond)*, 2007, **4**, 24.
28. E. Zannini, A. W. Sahin and E. K. Arendt, Resistant Protein: Forms and Functions, *Foods*, 2022, **11**.
29. R. F. Hurrell, M.-A. Juillerat, M. B. Reddy, S. R. Lynch, S. A. Dassenko and J. D. Cook, Soy protein, phytate, and iron absorption in humans, *The American journal of clinical nutrition*, 1992, **56**, 573-578.
30. I. C. Mayer Labba, M. Hoppe, E. Gramatkovski, M. Hjellström, M. Abdollahi, I. Undeland, L. Hulthén and A. S. Sandberg, Lower Non-Heme Iron Absorption in Healthy

Females from Single Meals with Texturized Fava Bean Protein Compared to Beef and Cod Protein Meals: Two Single-Blinded Randomized Trials, *Nutrients*, 2022, **14**.

31. T. Awosika and R. E. Aluko, Enzymatic Pea Protein Hydrolysates Are Active Trypsin and Chymotrypsin Inhibitors, *Foods*, 2019, **8**, 200.
32. S. Devaraju, P. Thatte, J. Prakash and J. A. Lakshmi, Bioaccessible iron and zinc in native and fortified enzyme hydrolyzed casein and soya protein matrices, *Food Biotechnology*, 2016, **30**, 233-248.
33. A. Dostal, C. Lacroix, V. T. Pham, M. B. Zimmermann, C. Del'homme, A. Bernalier-Donadille and C. Chassard, Iron supplementation promotes gut microbiota metabolic activity but not colitis markers in human gut microbiota-associated rats, *British Journal of Nutrition*, 2014, **111**, 2135-2145.
34. C. Poveda, D. I. Pereira, M. C. Lewis and G. E. Walton, The impact of low-level iron supplements on the faecal microbiota of irritable bowel syndrome and healthy donors using in vitro batch cultures, *Nutrients*, 2020, **12**, 3819.
35. G. T. Macfarlane and S. Macfarlane, Bacteria, colonic fermentation, and gastrointestinal health, *Journal of AOAC International*, 2012, **95**, 50-60.
36. C. Ceccarani, G. Bassanini, C. Montanari, M. C. Casiraghi, E. Ottaviano, G. Morace, G. Biasucci, S. Paci, E. Borghi and E. Verduci, Proteobacteria Overgrowth and Butyrate-Producing Taxa Depletion in the Gut Microbiota of Glycogen Storage Disease Type 1 Patients, *Metabolites*, 2020, **10**.
37. N. Gasaly, M. A. Hermoso and M. Gotteland, Butyrate and the fine-tuning of colonic homeostasis: implication for inflammatory bowel diseases, *International Journal of Molecular Sciences*, 2021, **22**, 3061.
38. A. Dostal, C. Chassard, F. M. Hilty, M. B. Zimmermann, T. Jaeggi, S. Rossi and C. Lacroix, Iron depletion and repletion with ferrous sulfate or electrolytic iron modifies the composition and metabolic activity of the gut microbiota in rats, *The Journal of nutrition*, 2012, **142**, 271-277.
39. A. Dostal, C. Lacroix, L. Bircher, V. T. Pham, R. Follador, M. B. Zimmermann and C. Chassard, Iron modulates butyrate production by a child gut microbiota in vitro, *mBio*, 2015, **6**, e01453-01415.
40. K. Oliphant and E. Allen-Vercoe, Macronutrient metabolism by the human gut microbiome: major fermentation by-products and their impact on host health, *Microbiome*, 2019, **7**, 91.
41. F. Blachier, F. Mariotti, J.-F. Huneau and D. Tomé, Effects of amino acid-derived luminal metabolites on the colonic epithelium and physiopathological consequences, *Amino Acids*, 2007, **33**, 547-562.
42. Y. Horimoto, R. Tan and L.-T. Lim, Enzymatic treatment of pork protein for the enhancement of iron bioavailability, *International Journal of Food Sciences and Nutrition*, 2019, **70**, 41-52.
43. L. Wang, S. Song, B. Zhang, C. Ai, C. Wen, Y. Gong, L. Jiang, Z. Sun, Y. Han and H. Xiao, A sulfated polysaccharide from abalone influences iron uptake by the contrary impacts of its chelating and reducing activities, *International Journal of Biological Macromolecules*, 2019, **138**, 49-56.
44. Y. Seyoum, K. Baye and C. Humblot, Iron homeostasis in host and gut bacteria – a complex interrelationship, *Gut Microbes*, 2021, **13**, 1874855.
45. F. Carbonero, A. C. Benefiel, A. H. Alizadeh-Ghamsari and H. R. Gaskins, Microbial pathways in colonic sulfur metabolism and links with health and disease, *Front Physiol*, 2012, **3**, 448.

46. K. Shatalin, E. Shatalina, A. Mironov and E. Nudler, H_2S: A Universal Defense Against Antibiotics in Bacteria, *Science*, 2011, **334**, 986-990.
47. D. Dordević, S. Jančíková, M. Vítězová and I. Kushkevych, Hydrogen sulfide toxicity in the gut environment: Meta-analysis of sulfate-reducing and lactic acid bacteria in inflammatory processes, *Journal of advanced research*, 2021, **27**, 55-69.

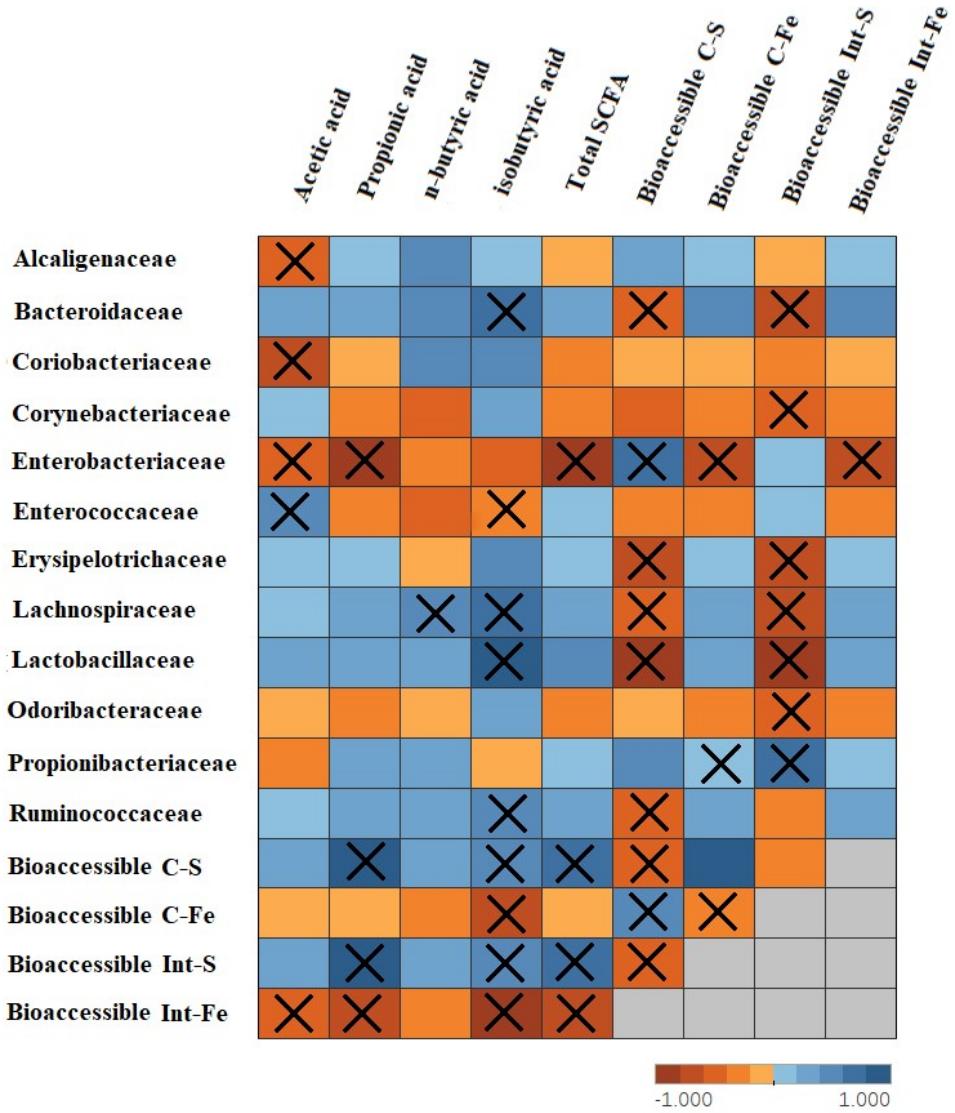

Figure 1. Spearman's pairwise correlation heatmap between normalized abundances of bacterial families and bioaccessible iron and sulfur. C. and Int. respectively represent colonic and intestinal stages. The gradient between red and blue indicates the scale of correlation between negative to positive. Squares with cross (X) indicate statistically significant (FDR-adj P < 0.05) values.

205x229mm (96 x 96 DPI)

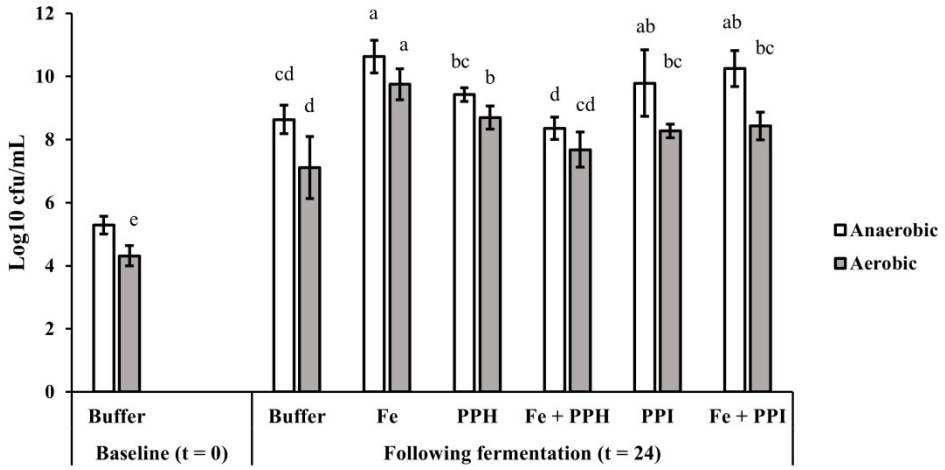

Figure 2. Total anaerobic and aerobic plate counts of the colonic fermented samples before and after 24 h (n = 3). Columns with different superscript letters within each condition (anaerobic or aerobic) are significantly different ($P < 0.05$). Buffer: culture with basal medium, Fe: iron salt control, PPH: pea hydrolysate, PPI: pea protein isolate, Fe + PPH: pea hydrolysate fortified with iron, Fe + PPI: pea isolate fortified with iron.

512x261mm (120 x 120 DPI)

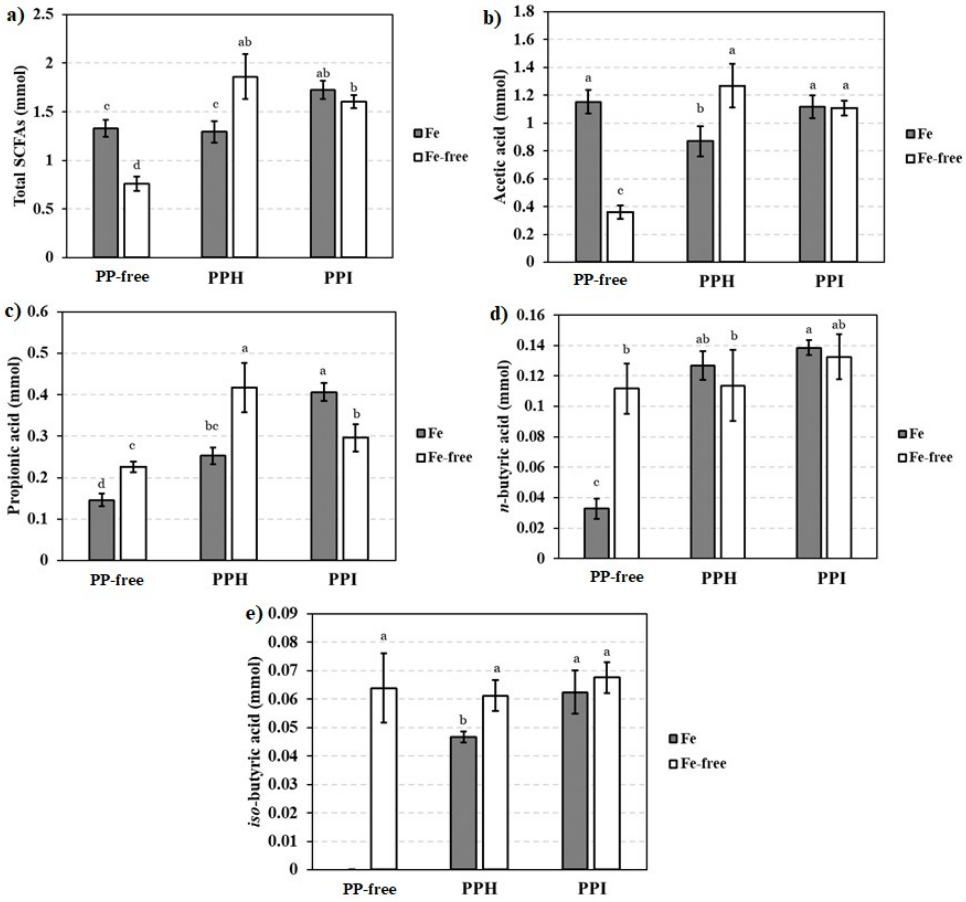

Figure 3. Short-chain fatty acids (SCFAs) produced in each treatment with and without fortified iron (Fe and Fe-free, respectively) after 24 h of colonic fermentation. a) total SCFAs, b) acetic acid, c) propionic acid, d) n-butyric acid, and e) iso-butyric acid. Values were expressed as means ± SD (n = 3), where treatment groups that do not share a superscript letter are significantly different ($P < 0.05$). PP-free: fermented culture without pea proteins, PPH: pea hydrolysate, PPI: pea protein isolate.

191x176mm (120 x 120 DPI)

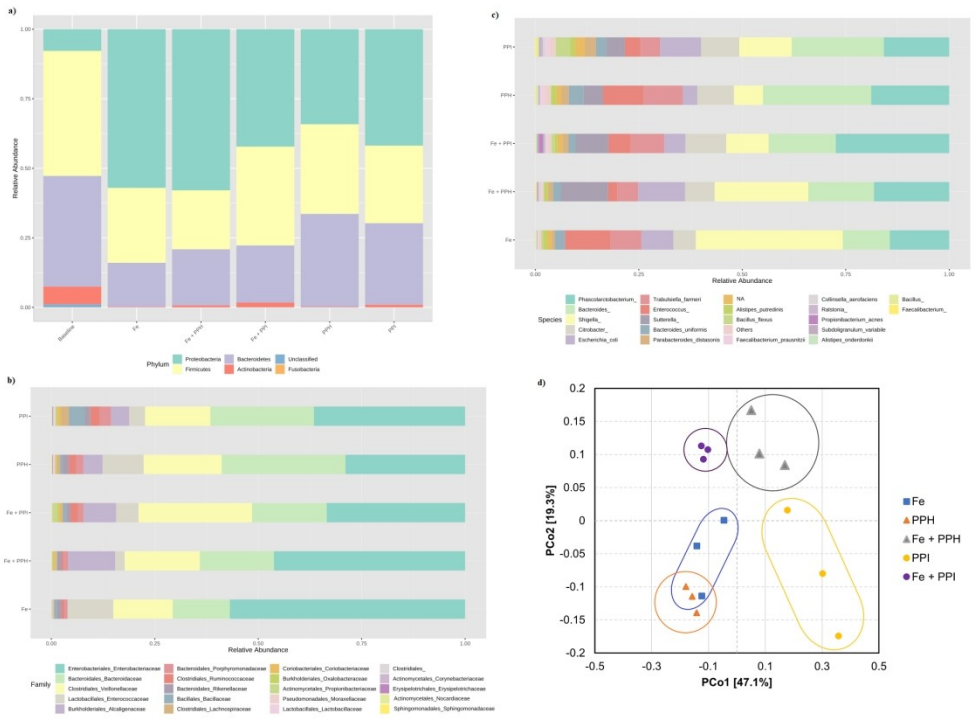

Figure 4. a) Top five phylum-level changes in the gut microbiome of the fermented samples versus the unfermented baseline culture ('Baseline'), with the remainder phyla merged in the 'Unclassified' group. b) and c) displays the top 20 families (prepended by order) and genus (including species where applicable) found in the microbiome of the fermented samples by relative abundance. d) Principal Coordinate Analysis (PCoA) plot as a β-diversity index of the gut microbiome profiles, based on Bray–Curtis dissimilarity between samples at a feature (OTU) level. Each data point represents the microbial community composition of one sample. All values excluding the PCoA plot are merged means of triplicates. Fe: iron salt control, PPH: pea hydrolysate, PPI: pea protein isolate, Fe + PPH: pea hydrolysate fortified with iron, Fe + PPI: pea isolate fortified with iron.

452x329mm (120 x 120 DPI)

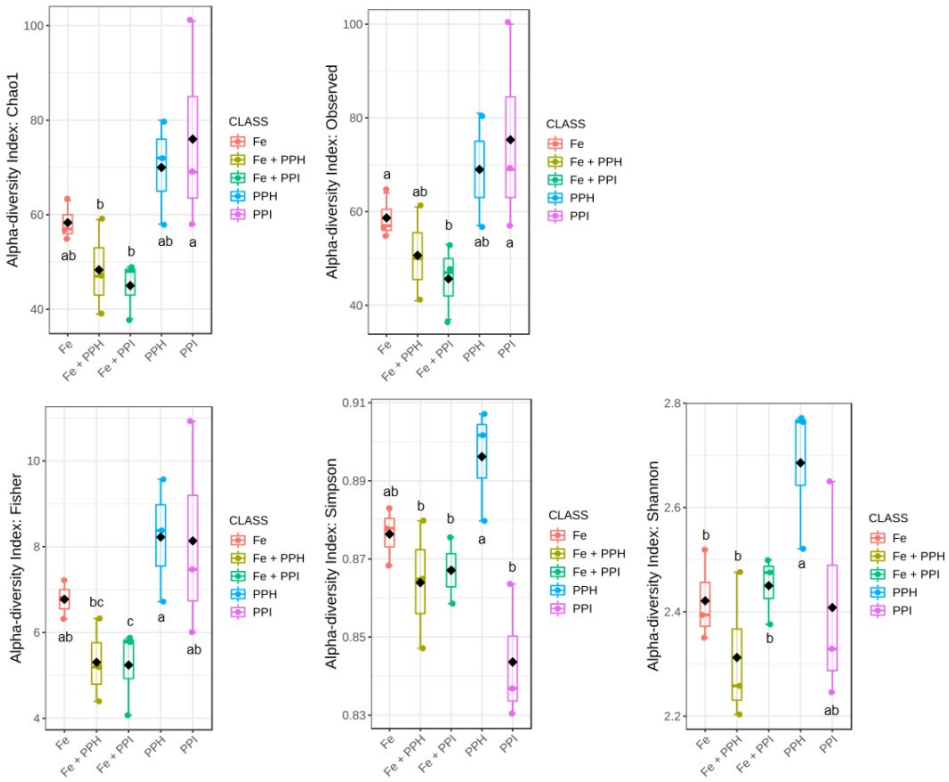

Figure 5. The α-diversity indices of the gut microbiome in the Fe salt control (Fe), pea hydrolysate (PPH), pea protein isolate (PPI), and the latter two groups fortified with iron (Fe + PPH, Fe + PPI). Analyses were conducted at the feature (OTU) level, where treatment groups that do not share a super/subscript letter are significantly different ($P < 0.05$).

237x191mm (120 x 120 DPI)

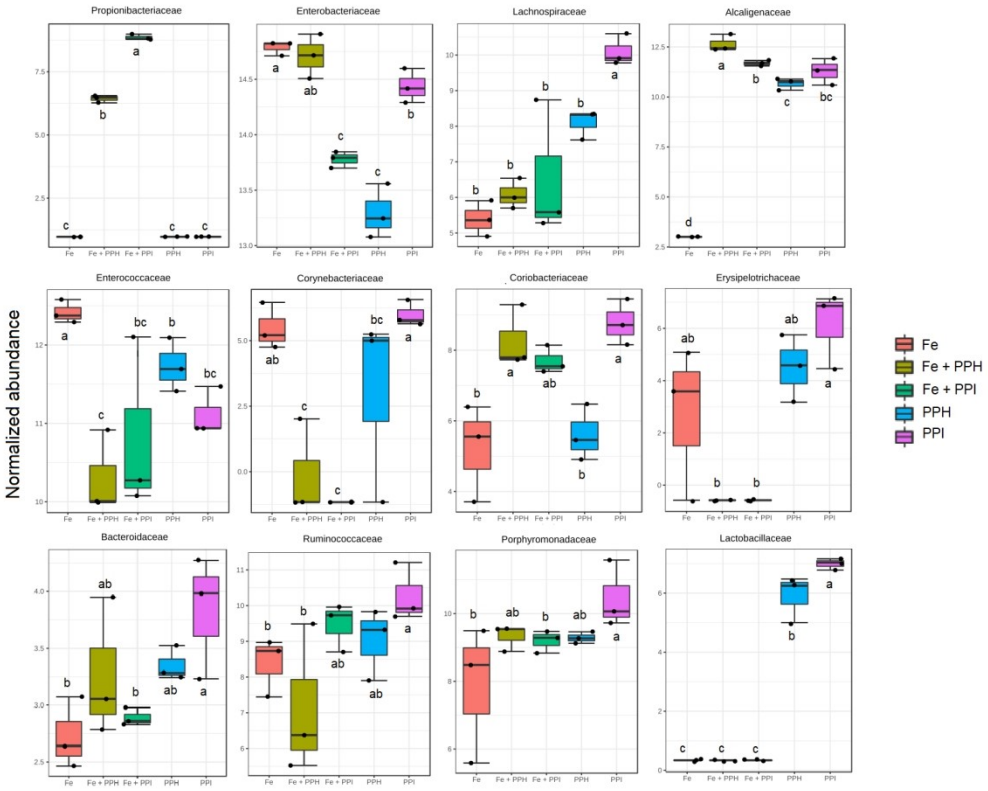

Figure 6. Boxplot of the abundances of 12 significantly different bacterial families as identified from ANOVA, where treatment groups that do not share a super/subscript letter are significantly different ($P < 0.05$). *Bacteroidaceae* and *Porphyromonadaceae* were no longer significant after adjusting for FDR. Fe: iron salt control, PPH: pea hydrolysate, PPI: pea protein isolate, Fe + PPH: pea hydrolysate fortified with iron, Fe + PPI: pea isolate fortified with iron.

342x276mm (120 x 120 DPI)